Aptasensors based on silicon nanowire field-effect transistors for electrical detection of thrombin

Valerie Stambouli, Guillaume Nonglaton, Rony Midahuen, Caroline Fontelaye, Nicolas Spinelli, Sylvain Barraud

Aptasensors based on silicon nanowire field-effect transistors for ~~reproducible~~ electrical detection of thrombin

Rony Midahuen[1], Valérie Stambouli[2], Caroline Fontelaye[1], Guillaume Nonglaton[1], Nicolas Spinelli[3], and Sylvain Barraud[1]

[1]Univ. Grenoble Alpes, CEA, LETI, 38054 Grenoble, France.

[2]Univ. Grenoble Alpes, CNRS, Grenoble-INP, LMGP, 38000 Grenoble, France

[3]Univ. Grenoble Alpes, CNRS, DCM UMR 5250, 38000 Grenoble, France

Corresponding author: Valérie Stambouli (e-mail: valerie.stambouli-sene@grenoble-inp.fr)

Abstract

Arrays of silicon nanowire field-effect transistors (Si NWFETs) were built to detect thrombin (a model biomarker) electrically. The Si NWFETs were created using a conventional top-down CMOS process, allowing them to be co-integrated with CMOS readout circuits in the future. EHTES organosilane was then used to graft aptamer probes onto the HfO_2 gate oxide of Si nanowires. We investigated the influence of aptamer grafting and thrombin recognition on the electrical transfer capabilities of Si NWFET aptasensors in details. Our technique was evaluated on a significant number of Si NWFETs, including two distinct chips with 30 aptasensors apiece. According to the findings, aptamer grafting increased the threshold voltage by a positive range of +28.8 mV to +87.7 mV, depending on the aptasensor employed. Thrombin identification, on the other hand, resulted in a negative shift of the threshold voltage between -26.6 and -23.8 mV. These opposing voltage shifts coincide with the aptamer probes' and thrombin molecules' electric charges, respectively. These findings provide unique demonstration of Si NWFETs manufactured utilizing typical top-down CMOS processing methods, allowing these devices to be used in various biomedical and biosensing applications.

Keywords : Si nanowire, thrombin, aptamer, aptasensor, CMOS

1. Introduction

Biosensors employing aptamer probes are identified as aptasensors. Aptamers [1, 2] are short oligonucleotide sequences (~15 to 60 nucleotides) selected so that they have affine and specific recognition properties for a given target molecule: proteins, small molecules of interest, macromolecules, etc. Unlike antibodies, aptamers which are chemically synthesized [3] have many advantages: small size, ease of conjugation with functional groups, stability to pH variations, reversible three-dimensional folding, and low manufacturing cost [4].

As part of this study, we used an aptamer specific to thrombin [5, 6], i.e. “thrombin binding aptamer” (TBA), to target the thrombin. This aptamer, which is suspended in a neutral buffer solution, adopts a three-dimensional conformation known as G-quadruplex that is approximately 2 nm in diameter [7]. Such a structure provides a specific probe function with a relatively low dissociation constant K_D of approximately 100 nM [6], in the presence of other competitive molecules which also have complexation affinities with thrombin. Thrombin is a protease of 295 amino acids [4, 8], the diameter of which is approximately 7 nm [9]. *In vivo*, the thrombin plays a central role in hemostasis and particularly in blood coagulation/anticoagulation metabolisms [10], in several cardiovascular diseases, and in the development of certain tumors. For example, the disease of venous thromboembolism, responsible for approximately 10.000 annual deaths in France [11] is due to a deregulation of the metabolic pathway of thrombin. Therefore, monitoring the blood level of so-called “active” thrombin in a patient is of crucial interest for the prevention and diagnosis of potential hemostatic abnormalities [12].

In view of biosensor fabrication for the detection of protein biomarker, especially thrombin in our case, there is a need for an instrumentation easily accessible, dedicated to the rapid and reliable measurement of circulating protein levels in the blood of a patient in care.
Ion Sensitive Field Effect Transistors (ISFETs) based on Si nanowires (Si NWFETs) have been intensively studied and developed over the last two decades due to many advantages of Si NWs in terms of highly controlled properties and fabrication processing. Indeed, combining unique tunable semiconducting properties with a high surface to volume ratio, Si NWs show an extreme sensitivity of their charge carriers to any modification of their surface potential induced by the presence of charged species [13]. For instance, DNA detection could be performed with Si NWFETs of 20 nm diameter with a low limit of detection (10 fM) [14]. Moreover, the wafer scale fabrication of Si NWFETs is compatible with an industrial mass production of existing semiconductor manufacturing companies. This enables a high integration of sensing devices suited for highly multiplexing and high-speed sampling. For these reasons, Si NWFETs are promising tools for portable, label-free, real time, selective and highly sensitive electrical measurements for biosensing applications. This is attested by reviews summarizing advances on Si NW-FETs made of parallel Si NW arrays patterned by top-down or bottom up approaches [15-17].

	Transducor	**Gate oxide**	**Functionalization agent**	**Reference electrode**	**LoD (detection limit)**	**Detection range**	**Ref.**
Organic FET	Au NP decorated bithiophène	--	Direct adsorption of thiolated apatamer probes on Au NPs	Si back gate	100 pM	0.1-100 nM	Hammock *et al*. [9]
	Graphene Bottom up	--	Butyric acid/NHS/PBASE	In plane integrated gate	2.6 pM	1 pM-1 µM	Kahn *et al*. [21]
Si NW FET	Single NW Bottom up p-type	SiO_2	3-aminopropyl diethoxy silane (APDES)	Pt	330 pM	--	Kim *et al.* [22]
	Multi NWs Bottom up Non doped	Al_2O_3	Glycidoxypropyl trimethoxysilane (GOPMS)	Ag/AgCl	200 pM	0.2-200 nM	Ibarluccea et *al.* [23]
	Multi NWs Top down Non doped	HfO_2	5,6-epoxyhexyl triethoxysilane (EHTES)	Ag/AgCl	-	2.7 µM	This work

Table 1. *Summary of thrombin detection on both organic and Si nanowire field-effect transistors.*

If the electrochemical detection of thrombin has been widely studied using amperometric and impedimetric aptasensors [18-20], only few groups have reported electrical systems for the detection of thrombin using NWFET functionalized with aptamers, i.e. aptaNWFETs. Most of these studies are reported in Table 1. They can be separated in two groups depending on the FET sensing nanomaterial: organic or Si NWs. BioFETs based on organic material ("Organic FET") were used by M. Hammock *et al.* [9] to perform real-time detection of thrombin molecules in a concentration range from 0.1 to 100 nM. N. Khan *et al.* [21] have implemented graphene-sheet BioFET chips with miniaturized microfluidic module making them entire portable instruments suitable for real-time measurement of low concentrations of thrombin with a detection limit of 2.6 pM. However, organic NWFETs are not very compatible with Si electronic industry, which is more suited to the fabrication of Si NWFET. To our knowledge, very few studies demonstrated an electrical detection of thrombin carried out with Si NWFET structures. K.

S. Kim *et al.* [22] developed a Si nanowire BioFET for the measurement of thrombin, concentrated to a few hundred of pM. The work of B. Ibarlucea *et al.* [23] involved BioFET chips based on Si nanowire arrays (up to 103 nanowires per transistor) coupled with a microfluidic system to perform real-time thrombin detection assays, in concentration ranges of clinical interest (from 0.2 to 200 nM). Both of these groups implemented a bottom up approach involving the vertical growth of Si NWs and then their transfer on the FET devices. In such processing configuration, the variability in NW characteristics induced by a bad control of dimensions and location, and a low metal contact quality can affect the reproducibility of electrical detection signals making this bottom up process very challenging [16, 24]. This is why a statistical study resulting from a wide range of devices is preferable to enable a better measurement reliability. To our knowledge, no other group has demonstrated thrombin detection using top down Si NWFETs even if this fabrication technique offers a better control of NW size, shape and geometry with a better yield allowing the scale-up of manufacturing.

In this study, for the first time, we present electrical detection of thrombin using a top down fabrication of Si NWFETs enabling a future CMOS integration.

In a previous work, we have presented our biologically sensitive Si NWFETs, fabricated at wafer scale, for pH sensing and the label-free detection of DNA hybridization [25]. The Si NWFETs were obtained using conventional top down CMOS processing technology. They have been designed with a wide range of widths and lengths as well as various dimensions of opening access for liquid introduction. The fabrication process was validated through the pH response measurement. A pH voltage sensitivity rising up to 600 mV/pH was obtained thanks to dual gate biasing mode involving both the reference electrode and the back gate [25]. Then, in a following step, electrical detection of DNA hybridization was performed thanks to a functionalization process of the Si NWFETs that was optimized to covalently graft DNA probes on the HfO_2 gate oxide covering the Si NW surface. This optimization was assessed by comparing two organosilanes: 5,6-epoxyhexyltriethoxysilane (EHTES) versus aminopropyltriethoxy silane (APTES). EHTES was selected for its better surface homogeneity, which is an important parameter to have reproducible detection results. Finally, DNA hybridization resulted in a significant increase of threshold voltage (+170 mV) in comparison to the non-complementary ssDNA grafted control devices. This is explained by the negative charges of DNA sequences [25].

Based on this optimized EHTES functionalization process, we fabricated Si NWFET aptasensors, i.e. Si aptaNWFETs, by grafting aptamer probes on the HfO_2 gate oxide. Then, we carried out electrical detection of thrombin. More particularly, we have thoroughly investigated the impact of both aptamer grafting and thrombin recognition on the transfer characteristics of the Si aptaNWFETs. We followed the evolution of transfer characteristics on a wide range of Si aptaNWFETs involving two independent chips constituted of 30 aptasensors. This allowed a deep statistical analysis of measurements. We show that aptamer grafting induces a positive shift of threshold voltage whereas the thrombin recognition induces a negative shift of threshold voltage. These results are consistent with the electric charges brought by the aptamer and the thrombin molecules respectively.

2. Material and methods

2.1 Si NWFET fabrication

The BioFETs (Si NWFETs) chips were fabricated from silicon-on-insulator (SOI) substrates. Fig. 1 shows a micrograph of two chips constituted of 250 BioFETs.

The technological fabrication steps have been previously described [25]. Briefly, they consist in using standard process steps of microelectronics such as photolithography, etching, deposition and planarization. We patterned multiple designs by means of hybrid deep ultraviolet (DUV) and electron-beam lithography followed by a reactive ion etching. Nanowires width down to 30 nm were achieved. Then, after the formation of contacts and metal lines, an additional step of lithography followed by an etching of SiO_2 layer were performed to open the Si NW test sites. These access opening were scaled down to 120 nm.

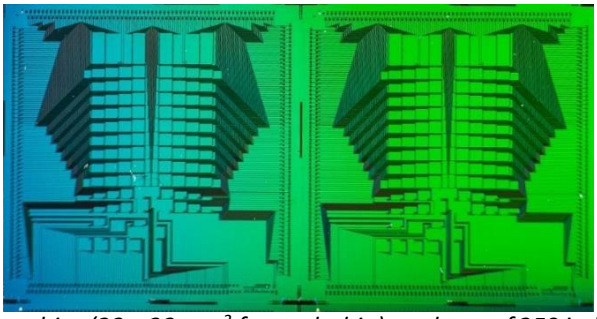

***Figure 1**. Photograph of two chips (22 × 22 mm² for each chip) made up of 250 independent Si NWFETs after performing all the fabrication steps.*

In this work, a part of each chip was selected (yellow rectangle of the chip layout as shown in Fig. 2a and b) in which 30 identical sensors were used to reproduce experiences and promote statistical studies. An array of 15 Si NWs (of 150 nm width and 1.5 µm length) can be seen inside microfluidic cavity (of 1.5 µm width and 8.5 µm length) (Fig. 2c). This is through this opening access to the test site that the Si NW arrays could be functionalized with aptamer grafting and then immerged in the electrolyte for electrical detection of protein, as schematized in Fig. 3d.

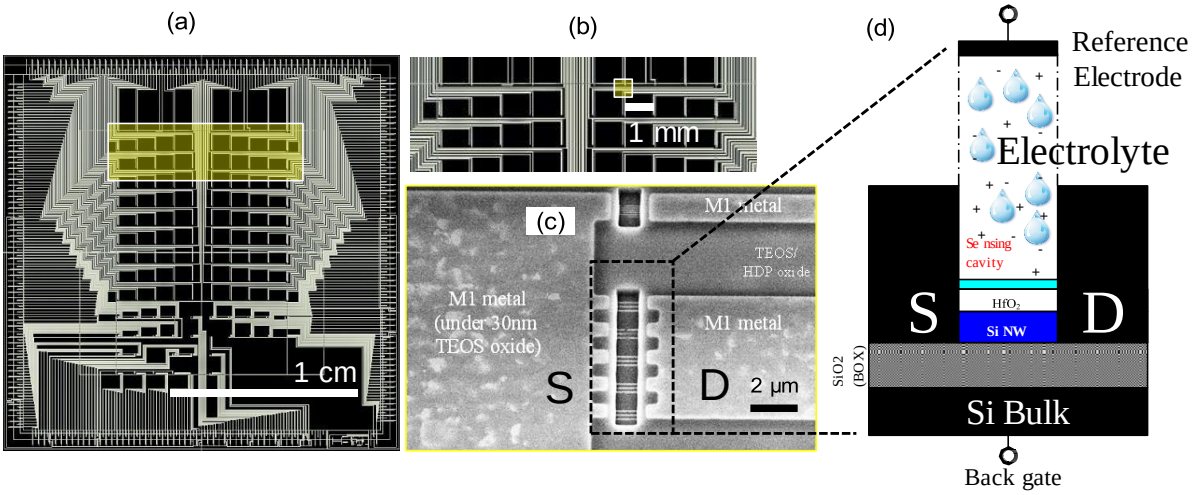

***Figure 2.** (a) Layout of our chip, (b) Region containing identical bioFETs organized in a matrix and spaced of one millimeter from each other. The white lines represent the metal lines of the bioFETs. These lines connect the devices to the pads located in the periphery of the chip, (c) SEM top view image of a cavity showing a bioFET including an array of 15 Si NWs connected between the source S and the drain D (d) Schematics of a bioFET with the electrolyte inside the microfluidic cavity and the aptamer layer (clear blue) grafted on HfO_2 oxide.*

Electrical characterization of devices in dry conditions showed typical transfer characteristics of n-MOSFETs with an I_{ON}/I_{OFF} ratio higher than 10^5 [25].

2.2 Functionalization of Si NWFETs

The covalent grafting of aptamer probes on the HfO_2 gate oxide of Si NWs was performed after the deposition of epoxy terminated organosilane "5,6-epoxyhexyltriethoxysilane" (EHTES). The main steps of EHTES functionalization protocol performed in liquid phase are illustrated in Fig. 3.

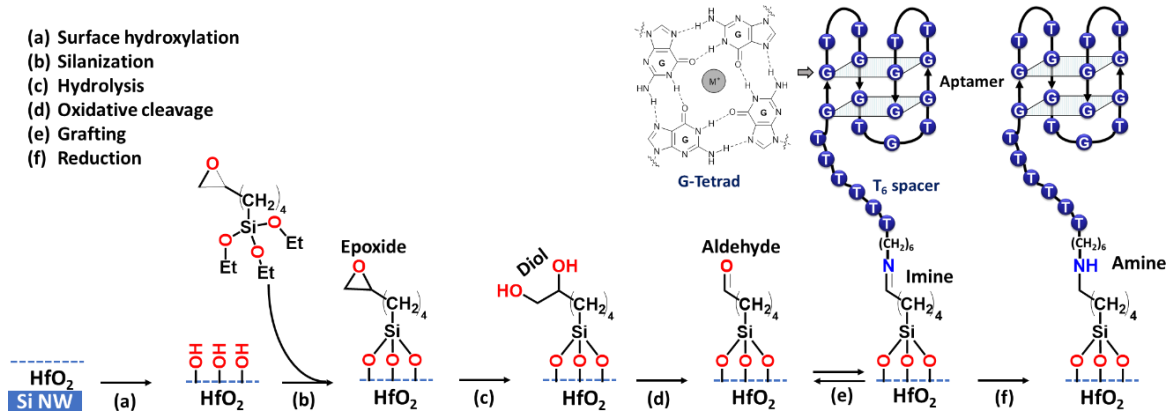

Figure 3. *Main steps of EHTES functionalization protocol on HfO_2 gate oxide. (a) hydroxylation using O_2 plasma, (b) EHTES silane liquid phase deposition, (c) hydrolysis of terminal epoxy end group into diol group, (d) oxidation of diol group into aldehyde group, (e) deposition of a 20 µL volume drop of TBA aptamer (C: 10 µM) for aptamer grafting resulting in an imine bond (f) reduction of imine double bond into amine single bond.*

After surface cleaning and hydroxylation enabling the creation of pending "OH" hydroxyl radicals on the surface of HfO_2 gate oxide (Fig. 3a), the samples were ready for EHTES deposition (Fig. 3b). They were immersed into a sealed vial containing 0.12% EHTES silane and 3.4% triethylamine diluted in toluene, and baked at 80°C for 16 hours. This was followed by rinsing steps to remove unbound reagents and by an annealing session for dehydration. Then, the epoxy terminals of EHTES were hydrolyzed into diols terminals (Fig. 3c) during a chemical reaction where the samples were immersed into a 5% sulfuric acid solution (H_2SO_4) for 2 hours. Then, the formation of aldehyde terminals (Fig. 3d) was carried out immersing the samples into a solution of 0.1 M sodium periodate ($NaIO_4$). The obtained aldehyde groups could react with the NH_2 termination of the thrombin binding aptamer (TBA) aptamer probes (Fig. 3e). The TBA aptamer probe molecules (5' H_2N-$(CH_2)_6$-T_6-GGTTGGTGTGGTTGG 3') were synthetized (DCM, UGA, France) with an amine termination in the 5' position. They were diluted to a concentration of 10 µM in a 10 mM Tris-HCl buffer pH 7.4 (1.5125 g/L of "Tris" reagent, supplemented with K^+ ions (0.0625 g/L) whose pH was adjusted from an HCl solution to the value of 7.4). The K^+ ions were added to the solution so that the folding reaction of the aptamers in the quadruplex structure was made possible [26].

The grafting of aptamer probes on the EHTES was carried out manually with a micropipette. A deposition of 20 µL drop of the aptamer probe solution on the surface of the chip is performed to cover the surface of the BioFETs and fill the cavity. The solution migrated by capillarity within this cavity, to be into contact with the surface of the silanized HfO_2 gate oxide and reacts with it. The chips were stored in a closed crystallizer at high humidity for 48 hours, during which the grafting of the aptamer probes on the silane layer took place by the formation of imine bonds bridging aptamers to the silane layer (Fig. 3e). After aptamer grafting, a rinsing of the samples with deionized water was carried out. The reduction of imine double bonds into more stable amine single bonds (Fig. 3f) was done immersing the chips in a solution of $NaBH_4$ (60 min, at room temperature). Finally, the samples were rinsed with sodium dodecyl sulfate (SDS) detergent (0.2%), followed by several rinses carried out with deionized water.

The freeze-dried human α-thrombin molecules (Merck, France) were diluted to a concentration of 2.7 µM in a weakly concentrated sodium phosphate buffer (PBS) at 0.1 mM, pH = 5.4. An electrolyte with a low ion concentration reduces the screening effects of the charges contained in the electrolyte and therefore provide a better capacitive coupling between the biological charges of the electrolyte and the conduction channel of BioFETs [20, 21, 27].

Electrical detection of thrombin was performed by keeping the surface of the chips always wet and the reference electrode always immersed. The conjugation time of the thrombin to its aptamer was half an hour [28-29].

2.3 Wettability measurements

The water contact angle measurements were carried out using a Digidrop drop-shape analyzer (GBX instrument, France) at room temperature after the deposition of a 1 µL drop of deionized water on the surface of the HfO_2 gate oxide. The precision on the angle measurement is ±5°.

2.4 Electrical measurements

Electrical characterization of bioFETs (aptasensors) was carried out on a test station under probes connected to an analyzer (Semiconductor Parameters Analyzer HP4156A). The drain current I_{DS} was measured as a function of the voltage V_{REF} applied to an Ag/AgCl commercial reference electrode (WPI, USA) immersed in the electrolyte. V_{REF} was biased from 0.5 to 2 V with a step of 20 mV. The source voltage (V_S) and the back-gate voltage (V_{BG}) were fixed at 0 V. The drain voltage (V_{DS}) was fixed at 1 V. The electrical characterization was obtained in liquid medium (volume: 100 µL) after 4 key steps:

1. Before aptamer probe grafting (bare aptasensors) in sodium acetate buffer (C: 100 mM, pH 7).
2. After aptamer probe grafting in sodium acetate buffer (C: 100 mM, pH 7).
3. Before thrombin introduction in thrombin phosphate buffer (0.01× dilution buffer, pH 5.4, without thrombin).
4. After thrombin recognition（C: 2.7 µM) in thrombin phosphate buffer (0.01× dilution buffer, pH 5.4).

3. Results and discussion

3.1 Wettability measurement

The measurement of water contact angle performed at different functionalization steps enabled to have an indirect overview of chemical modifications of the surface. The water contact angles were measured at three main steps, i.e. after hydroxylation, after EHTES deposition and after aptamer grafting. The values are reported in Table 2. The contact angle started with a value close to 1° typical of the presence of pending hydroxyl groups. The latter induced a highly hydrophilic surface due to the cleaning and exposure of the HfO_2 oxide to the energetic gaseous plasma. Then, the definitive bonding of the silane layer on the HfO_2 surface was confirmed by a significant increase in the contact angle reaching 41°. Finally, the aptamer probe grafting step also induced an increase of +6.7° of contact angle. These measurements indicate successful attachment of the probes to the gate oxide surface of our bioFETs.

	Hydroxylation	Silanisation	Aptamer probe grafting
Schematic of surface state		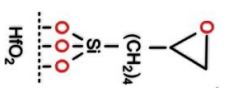	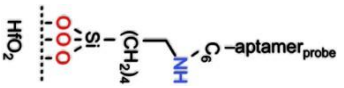
Contact angle value	~1°	~41°	~48°

Table 2. *Values of the water contact angle after the main steps of functionalization*

3.2 Electrical measurements

The measurements were performed on two independent chips (chip 1 and chip 2) having each 30 identical aptasensors (Fig. 1 and 2). Fig. 4 and 5 show typical examples of transfer characteristics of the same aptasensors obtained after the four functionalization key steps described previously, i.e. before

and after aptamer grafting (Fig. 4), then before and after thrombin recognition (Fig. 5). According to the step, different threshold voltage ΔV_t shifts were observed which are detailed in the following.

3.2.1 Effect of aptamer probe grafting

The aptasensor transfer characteristics were measured before ("bare HfO_2 surface") and after aptamer grafting on 6 representative aptasensors (Fig. 4). We observe that aptamer grafting induced a positive ΔV_t shift that is represented by a red arrow on the curves. More particularly, on chip 1, 27 over 30 aptasensors presented a positive average ΔV_t shift of +28.8 mV whereas on chip 2, 22 over 30 aptasensors exhibited a positive mean ΔV_t shift of +87.7 mV. These threshold voltage ΔV_t shifts indicate a change in the surface states of the HfO_2 gate oxide of aptasensors induced by the negative charges carried by the aptamer probe molecules.

For a same drain current I_{DS} measured in the sub-threshold regime of our aptasensors (10^{-8} A), the charges carried by the aptamer probes increased the electrode voltage value V_{REF} that is necessary for establishing the conduction channel. The positive V_t shift is explained by the "n-type" nature of the aptasensor used in this work. Quantitatively, on the first chip, 90% of the aptasensors met the criteria of higher threshold voltage induced by the aptamers grafting against 73.3% for the second chip. This difference in the average ΔV_t between the first and the second chip (+28.8 mV vs +87.7 mV respectively) can be explained by some manipulation biases during manual deposition of aptamer probe solutions on the chip surface. This solution might not be fully homogeneous, inducing a more concentrated deposition of aptamer probe molecules on the surface of the second chip.

For the following step, whose purpose was the thrombin recognition, we considered only the aptasensors having presented a positive response to aptamer grafting.

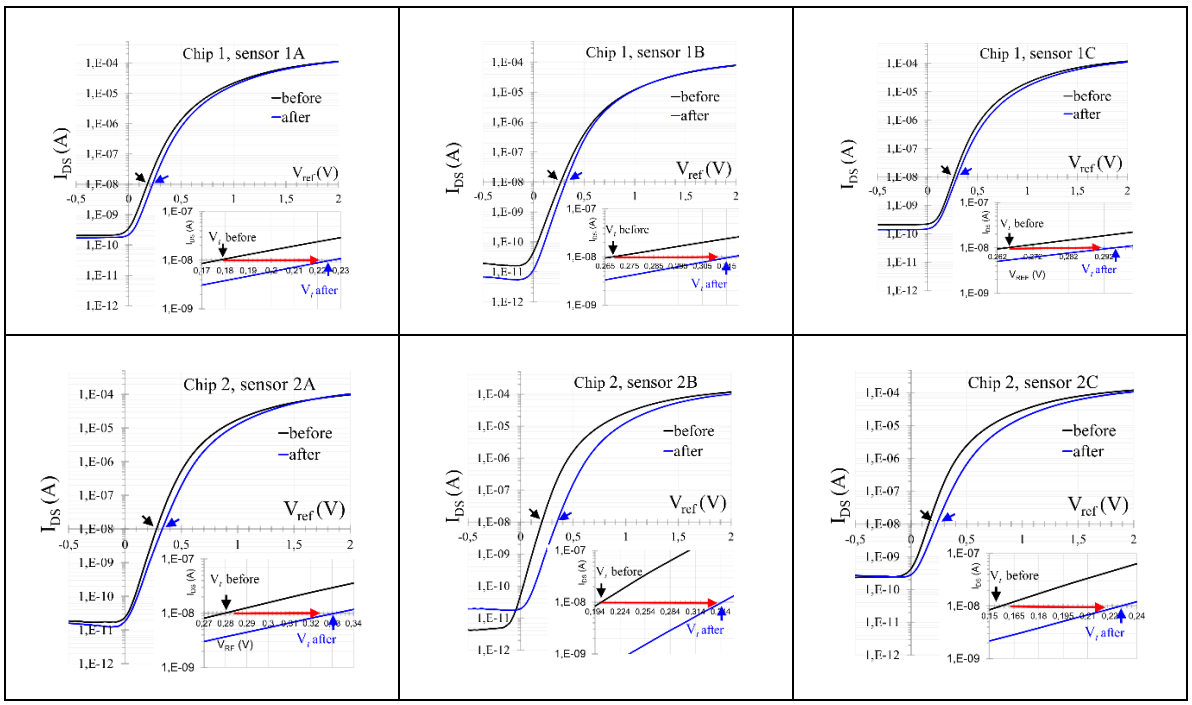

Figure 4. *Typical electrical characteristics I_{DS} as a function of V_{REF} (V_S and V_{BG}: 0V and V_{DS}: 1V) obtained before and after aptamer grafting on six aptasensors from two independent chips (chip 1 and chip 2 as shown in Fig. 1 and Fig.2).*

3.2.3 Effect of thrombin recognition

Following the same scheme as for the characterization of TBA aptamer probes grafting, the electrical measurements for thrombin detection were carried out in two steps. A first electrical measurement of aptasensors in the presence of a "blank" thrombin dilution buffer (thrombin concentration of 0 µM) which defined a reference curve before performing the same electrical measurement but in the presence of thrombin. Since thrombin has an isoelectric pHi (pH of electrical neutrality) between 7 and 7.6 [23], the pH of the dilution buffer was 5.4 in order to shift the thrombin charge balance towards a positive overall charge. The effects of the thrombin recognition on the electrical characteristics of the previous aptasensors of Fig. 4, are reported in Fig. 5. Compared to the reference measurements carried out without thrombin, the addition of thrombin induced a negative ΔV_t shift represented by a red arrow on the curves. More generally, a negative average ΔV_t shift of -26.6 mV was obtained on the first chip with 85% of aptasensors having a favorable response. On the second chip, 91% of aptasensors exhibited an average negative ΔV_t shift of -23.8 mV. Elsewhere, a similar trend showing negative shift of V_t upon thrombin detection was obtained by B. Ibarlucea *et al.* on Si NWFETs fabricated by bottom up process [23].

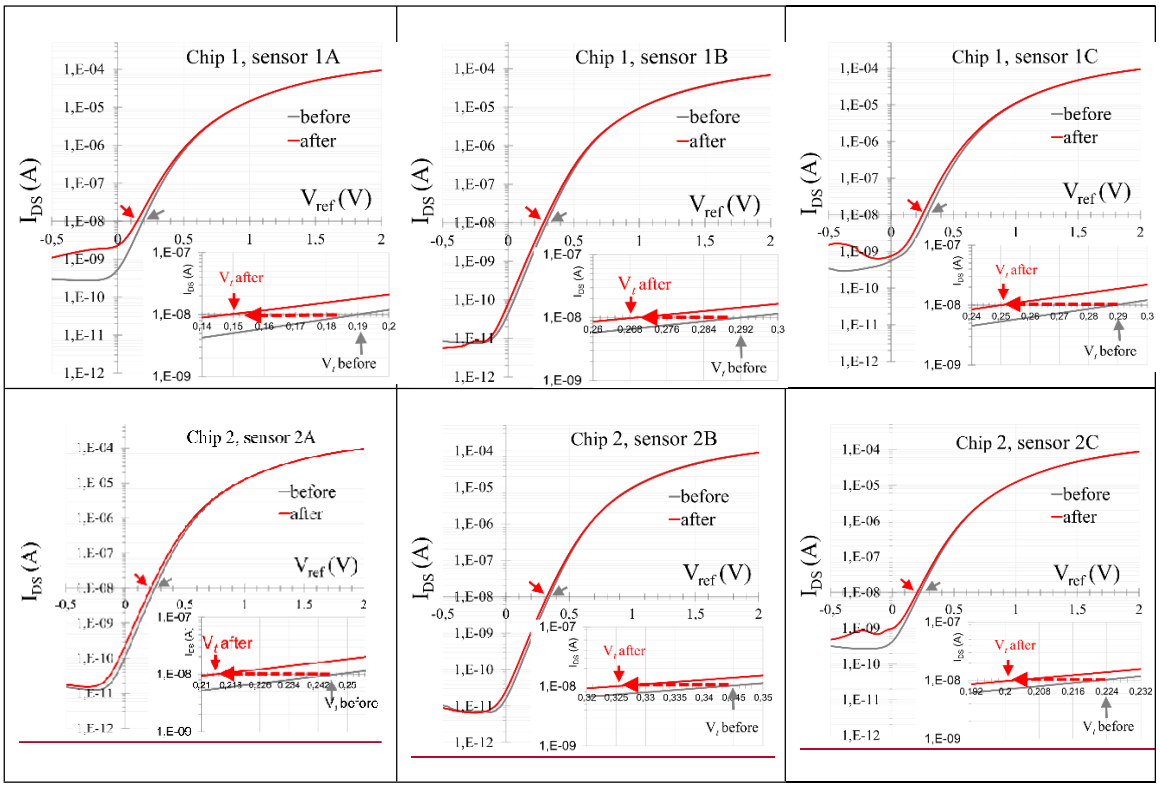

Figure 5. *Impact of thrombin recognition on the electrical characteristics I_{DS} as a function of V_{REF} (V_S and V_{BG} : 0V and V_{DS} : 1V) obtained on the six aptasensors previously shown in Fig. 4.*

Our results are consistent with the fact that in its dilution buffer, the thrombin is positively charged. The additional positive charges increase the electrostatic potential that is applied to the gate oxide of the aptasensors and further promote the creation of the underlying conduction channel. As a result, the threshold voltage V_t of the aptasensor was reduced. To visually assess both the intra-chip variability and dispersion of ΔV_t shift, box diagrams are presented after both aptamer grafting (Fig. 6a) and thrombin recognition (Fig. 6b). The latter was obtained based on ΔV_t values extracted from the electrical characteristics for all aptasensors of the two independent chips.

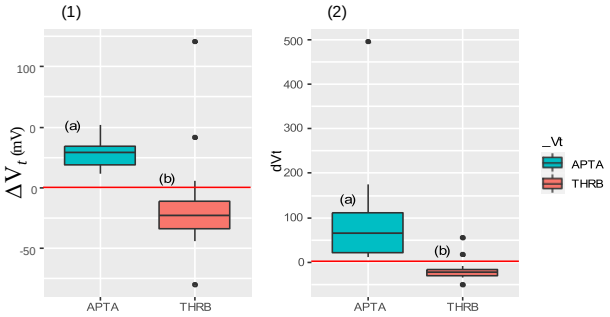

Figure 6. *Box diagrams presenting the ΔV_t shift extracted from the transfer characteristics of aptasensors of the first chip (1) and the second chip (2) upon the two steps: (a) after TBA aptamer grafting, (b) after thrombin recognition. The red line indicates the reference threshold voltage ΔV_t of the bare sensors (i.e. before aptamer grafting or before the introduction of thrombin).*

Compared to the reference threshold voltage of the bare sensors (red line in Fig. 6) and considering for error bars, the results show a positive shift of ΔV_t induced by aptamer grafting and a negative shift of ΔV_t induced after thrombin recognition. Similar results were achieved on the two independent chips. This demonstrates the reproducible and reliable sensing function in agreement with the negative or positive charges brought by the molecules located on the surface of our aptasensors.

3.2.2 Discussion

After TBA aptamer_probe grafting, the mean shift of threshold voltage is four times higher in chip 2 (from +28.8 mV to +87.7 mV), however both chips show limited Vth shift variability (from -26.6 mV to -23.8 mV) after the thrombin recognition. This higher variability following TBA grafting raises concerns for chips done under same conditions.

The effect of TBA_aptamer grafting on the transfer properties of a functionalized silicon surface has received little attention in the literature. There are various probable explanations in our example. This complexity concerns the development of the TBA molecular sequence, which is made up of two key parts: a T6 spacer located at the 5' end of the aptamer sequence and the G quadruplex. The G quadruplex configuration contains a planar tetrameric arrangement of guanine bases called G-tetrad (Fig. 3), which in turn can be stacked on top of each other, thank to π-π interactions, being stabilized by monovalent cations such as K^+ and Na^+ [30-33]. These structures may build different types of multimers, such as wires, stacks of intramolecular structures and interlocked dimers and trimers [34, 35]. In our case, it is likely that each of the two components of the TBA probes has a distinct role during the grafting process onto the silanized HfO_2/Si surface.

First, the T6 spacer allows for flexibility in the orientation of the G quadruplex, leading to different orientations of the aptamer probes on the surface. These orientations include standing, lying, and intermediate positions. This has been demonstrated from surface enhanced Raman spectroscopy (SERS) studies on aptamers immobilized of Au surfaces [36]. Thus, here, the various orientations of aptamers on the Si surface can influence the spatial distribution of negative charges and lead to different Vth shifts.

Secondly, we previously conducted an in-depth analysis of the process of TBA grafting and compared it to the process of single-strand DNA probes with comparable length to TBA on Si nanonetFETs (NNFETs) - that feature arrays of Si NWs - using the same TBA concentration [37]. Specifically, AFM analyses have demonstrated that TBA molecules created new structures or aggregates on the surface, while no such effect was observed with linear single strand DNA probes. These structures were identified as stackings of several TBA due to the strong π-π interactions between the G quadruplexes as described above. The presence of aggregates of TBA, along with single TBA molecules on the Si

surface, results in a non-uniform distribution of negative charges on the surface. Such distribution may vary between chips.

Besides, we have also shown that the TBA grafting effect on the transfer characteristics $I_d(V_{BG})$ is strongly time dependant [37]. It is required to wait between 24 and 48 hours for the system to stabilize. Indeed many metastable intermediate conformations can exist in the unfolding and folding pathway and what their structures are, depending on the physicochemical conditions in their micro-environment, including ionic concentration, pH and the chemistry [38, 39]. Here, a 48h stabilization time was respected for the I(V) measurements. However, the folding pathway conditions do not appear to be straightforward from chip to chip, and local differences in the TBA folding process may explain the high variability of the Vth shift.

All of these results highlight the fact that grafting TBA probes is not as simple as grafting linear single strand DNA probes. To increase the reproducibility of the Vth measurement, it must be carefully controlled and adjusted.

Taking these considerations into account and considering the shift of Vth upon the thrombin recognition by TBA probes, we could expect also a large variation of Vth shift. This is not the case because the data show very little variation. This can be explained by the observations from SERS studies made by Lamy *et al.* [36]. The interaction between thrombin and aptamer results in the formation of a TBA/thrombin complex that has distinctive structural rigidity and reduced aptamer flexibility. The protein freezes the aptamer conformation [36]. Thus this results in a reduced spatial variation of the charges on the Si surface. Besides, it is also probable that the structures (aggregates) of TBA are less involved in the thrombin recognition, or this phenomenon is maybe too far from the surface and cannot be sensed by the Si NW. These observations and hypotheses can explain the smaller Vth shift variation upon thrombin recognition compared to TBA grafting.

These hypotheses aim to explain these preliminary results. They suggest that controlling and optimizing the conditions for TBA grafting onto the silanized silicon surface is crucial for reducing electrical measurement variability. To achieve this, the effect of varying TBA concentration needs to be thoroughly studied to determine the optimum level. Once the optimal concentration has been determined, the impact of fluctuating thrombin concentration can be explored to evaluate the efficiency of our aptasensor in terms of sensitivity, limit of detection, and selectivity. Such research will form the basis of future studies. Furthermore, the use of microarray spotter can enable more precise, efficient and reproducible aptamer deposition.

4. Conclusions

The present study shows a proof of concept for electrical detection of thrombin on aptasensors that we have fabricated using standard CMOS compatible fabrication of Si NWFETs. Thanks to a high number of measurements on different Si NWFETs, a statistical study has been carried out demonstrating the reliability of our Si aptaNWFETs. The measured ΔV_t shift are in agreement with the chemical reaction occurring at the surface of NWs: a positive shift of ΔV_t induced by aptamer grafting, and a negative shift of ΔV_t induced after thrombin recognition. This early work paves the door for further investigations. They include the optimization of the TBA probe grafting process and notably TBA concentration onto the silanized HfO_2/Si surface in order to reduce the variability of the Vth shift. Then the impact of fluctuating thrombin concentration could be explored to evaluate the efficiency of our sensor in terms of sensitivity, limit of detection, and selectivity. Elsewhere, regarding the device operating mode, the use of the dual gate mode measurement combining efficiently the reference electrode bias with the back-gate bias could allow for an enhanced sensitivity while decreasing the detection limit.

Acknowledgements

The authors thanks M. Vallejo-Perez (LMGP and DCM, UGA, F) for aptamer molecules synthesis as well as B. Ibarlucea (UTB, Dresden, Germany) for fruitful discussions about thrombin pHi.

References

[1] E. J. Cho, J. W. Lee, A. D. Ellington, Applications of aptamers as sensors. Annu. Rev. Anal. Chem. 2 (2009) 241–64, doi:10.1146/annurev.anchem.1.031207.112851.

[2] A. B. Iliuk, L. Hu, W. A. Tao, Aptamer in bioanalytical applications. Anal. Chem. 83 (2011), 4440–445, doi:10.1021/ac201057w.

[3] R. Stoltenburg, C. Reinemann, B. Strehlitz, SELEX-A (r)evolutionary method to generate high-affinity nucleic acid ligands. Biomolecular Engineering 24 (2007) 381–403, doi:10.1016/j.bioeng.2007.06.001.

[4] B. Deng, Y. Lin, C. Wang, F. Li, Z. Wang, H. Zhang, X.-F. Li, X. Chris Le, Aptamer binding assays for proteins: The thrombin example-A review. Anal. Chim. Acta 837 (2014) 1-15, doi:10.1016/j.aca.2014.04.055.

[5] P.-H. Lin, R.-H. Chen, C.-H. Lee, Y. Chang, C.-S. Chen, W.-Y. Chen, Studies of the binding mechanism between aptamers and thrombin by circular dichroism, surface plasmon resonance and isothermal titration calorimetry. Colloids Surfaces B Biointerfaces 88 (2011) 552-558, doi:10.1016/j.colsurfb.2011.07.032

[6] D. M. Tasset, M.F. Kubik, W. Steiner, Oligonucleotide inhibitors of human thrombin that bind distinct epitopes. J. Mol. Biol. 272 (1997) 688-698, doi:10.1006/jmbi.1997.1275.

[7] H. Hasegawa, K. I. Taira, K.Sode, K. Ikebukuro, Improvement of aptamer affinity by dimerization. Sensors, 8 (2008) 1090-1098, doi:10.3390/s8021090.

[8] J.-O. Lee, H.-M. So, E.-K. Jeon, H. Chang, K. Won, Y. H. Kim, Aptamers as molecular recognition elements for electrical nanobiosensors. Anal. Bioanal. Chem. 390 (2008) 1023–1032, doi:10.1007/s00216-007-1643-y.

[9] M. L. Hammock, O. Knopfmacher, B. D. Naab, J. B. H. Tok, Z. Bao, Investigation of protein detection parameters using nanofunctionalized organic field-effect transistors. 7 (5) (2013) 3970–3980, doi:10.1021/nn305903q.

[10] J. T. B. Crawley, S. Zanardelli, C. K. N. K. Chion, D. A. Lane, The central role of thrombin in hemostasis. J Thromb Haemost 2007; 5 (Suppl. 1): 95–101. doi:10.1111/j.1538 7836.2007.02500.x.

[11] Oger, E. Incidence of venous thromboembolism: A community-based study in western France. Thromb. Haemost, 83 (2000) 657–60, doi:10.1055/s-0037-1613887.

[12] M. Adams, Assessment of thrombin generation: Useful or hype? Seminars in Thrombosis and Hemostasis, vol 35 (1) (2009) 104-10, doi:10.1055/s-0029-1214153.

[13] D. Sadighbayan, M. Hasanzadeh, E. Ghafar-Zadeh, Biosensing based on field-effect transistors (FET): recent progress and challenges, Trends in Analytical Chemistry 133 (2020) 116067, doi: 10.1016/j.trac.2020.116067

[14] M. N. Nuzaihan, U. huashim, M. K. Arshad, A. Rahim Ruslinda, S. F. Rahman, M. F. Fathil, M. H. Ismail, Top-Down Nanofabrication and Characterization of 20 nm Silicon Nanowires for Biosensing Applications, PLoS ONE 11(3) (2016) e0152318, doi:10.1371/journal.pone.0152318

[15] G.J. Zhang, Y. Ning, Silicon nanowire biosensor and its applications in disease diagnostics: A review. Anal. Chim. Acta 749 (2012) 1–15, doi: 10.1016/j.aca.2012.08.035

[16] R. Ahmad, T. Mahmoudi, M.S.Ahn, Y.B. Hahn, Recent advances in nanowires-based field-effect transistors for biological sensor applications. Biosens. Bioelectron. 100 (2018) 312–325, doi.org/10.1016/j.bios.2017.09.024

[17] D.P. Tran, T.T.T. Pham, B. Wolfrum, A. Offenhäusser, B. Thierry, CMOS-compatible silicon nanowire field-effect transistor biosensor: Technology development toward

commercialization. Materials 11 (2018) 785, doi:10.3390/ma11050785
[18] H. Xu, K. Gorgy, C. Gondran, A. Le Goff , N. Spinelli, C. Lopez , E. Defrancq and S. Cosnier, Label-free impedimetric thrombin sensor based on poly(pyrrole-nitrilotriacetic acid)-aptamer film. Biosens. Bioelectron. 41 (2013) 90 – 95, doi: 10.1016/j.bios.2012.07.044
[19] Z. Zhang, Shunli Liu, Yu Shi, Yuanchang Zhang, Dave Peacock, Fufeng Yan, Peiyuan Wang, Linghao He, Xiaozhong Feng and Shaoming Fang, Label-free aptamer biosensor for thrombin detection on a nanocomposite of graphene and plasma polymerized allylamine J. Mater. Chem. B, 2 (2014) 1530, doi: 10.1039/c3tb21464h
[20] A. Gosai, B. Shin Hau Yeaha, M. Nilsen-Hamilton, P. Shrotriya, Label Free Thrombin Detection in Presence of High Concentration of Albumin Using an Aptamer-Functionalized Nanoporous Membrane, *Biosens. Bioelectron.* 126 (2018) 88-95, doi:10.1016/j.bios.2018.10.010
[21] N. I. Khan, M. Mousazadehkasin, S. Ghosh, J. G. Tsavalas, E. Song, An integrated microfluidic platform for selective and real-time detection of thrombin biomarkers using a graphene FET. Analyst 145 (2020) 4494, doi:10.1039/d0an00251h.
[22] K. S. Kim, H. S. Lee, J. A. Yang, M. H. Jo, S. K. Hahn, The fabrication, characterization and application of aptamer-functionalized Si-nanowire FET biosensors. Nanotechnology 20 (2009) 235501-07, doi:10.1088/0957-4484/20/23/235501.
[23] B. Ibarlucea, L. Römhildt, F. Zörgiebel, S. Pregl, M. Vahdatzadeh, W. M. Weber, T. Mikolajick, J. Opitz, L. Baraban, G. Cuniberti, Gating hysteresis as an indicator for silicon nanowire FET biosensors. Appl. Sci. 8 (2018) 950, doi:10.3390/app8060950
[24] M. Tintelott, V. Pachauri, S. Ingebrandt, X.T. Vu, Process Variability in Top-Down Fabrication of Silicon Nanowire-Based Biosensor Arrays. Sensors 21 (2021) 5153. doi.org/10.3390/s21155153
[25] R. Midahuen, B. Previtali, C. Fontelaye, G. Nonglaton, V. Stambouli, and S. Barraud, Optimum functionalization of Si nanowire FET for electrical detection of DNA hybridization, J. Electron. Dev. Soc. 10 (2022) 575-583, doi:10.1109/JEDS.2022.3166683
[26] R. F. Macaya, P. Schultze, F. W. Smith, J. A. Roe and J. Feigon, Thrombin-binding DNA aptamer forms a unimolecular quadruplex structure in solution. Proc. Natl. Acad. Sci. 90(1993)3745-3749, doi:10.1073/pnas.90.8.3745.
[27] E. Stern, R. Wagner, F. J. Sigworth, R. Breaker, T. M. Fahmy, M. A. Reed, Importance of the Debye screening length on nanowire field effect transistor sensors. Nano Lett. 7 (2007) 3405–3409, doi: 10.1021/nl071792z
[28] A. Sosic, A. Meneghello, E. Cretaio, B. Gatto, Human thrombin detection through a sandwich aptamer microarray: Interaction analysis in solution and in solid phase. Sensors 11 (2011) 9426-9441, doi:10.3390/s111009426.
[29] A. Meneghello, A. Sosic, A. Antognoli, E. Cretaio, B. Gatto, Development and Optimization of a Thrombin Sandwich Aptamer Microarray. Microarrays 1 (2012) 95-106, doi:10.3390/microarrays1020095.
[30] V. Dapi, V. Abdomerovi, R. Marrington, J. Peberdy, A. Rodger, J.O. Trent, P.J. Bates, Biophysical and biological properties of quadruplex oligodeoxyribonucleotides. Nucleic Acids Res. 2003, 31, 2097–2107 doi: 10.1093/nar/gkg316.
[31] V.C. Diculescu, A.M. Chiorcea-Paquim, R. Eritja, A.M. Oliveira-Brett, Thrombin-binding aptamer quadruplex formation: AFM and voltammetric characterization. J. Nucleic Acids 2010, 2010, 841932. doi:10.4061/2010/841932
[32] A.M. Chiorcea-Paquim, P.V. Santos, R. Eritja, A.M. Oliveira-Brett, Self-assembled G-quadruplex nanostructures: AFM and voltammetric characterization. Phys. Chem. Chem. Phys. 2013, 15, 9117–9124, https://doi.org/10.1039/C3CP50866H
[33] T.C.Marsh, J. Vesenka, E. Henderson, A new DNA nanostructure, the G-wire, imaged by scanning probe microscopy. Nucleic Acids Res. 1995, 23, 696–700
[34] G. Oliviero, S. D'Errico, B. Pinto, F. Nici, P. Dardano, I. Rea, L. De Stefano, L. Mayol, G. Piccialli, N. Borbone, Self-assembly of g-rich oligonucleotides incorporating a 3'-3' inversion of polarity

site: A new route towards G-Wire DNA nanostructures. ChemistryOpen 2017, 6, 599–605. doi: 10.1002/open.201700024

[35] A.M. Varizhuk, A.D. Protopopova, V.B. Tsvetkov, N.A. Barinov, V.V. Podgorsky, M.V. Tankevich, M.A. Vlasenok, V.V. Severov, I.P. Smirnov, E.V. Dubrovin, *et al.* Polymorphism of G4 associates: From stacks to wires via interlocks. Nucleic Acids Res. 2018, 46, 8978–8992. doi: 10.1093/nar/gky729

[36] W. Safar, A.-S. Tatar, A. Leray, M. Potara, Q. Liu, M. Edely, N. Djaker, J. Spadavecchia, W. Fu, S. Gam Derouich, N. Felidj, S. Astilean, E. Finot and M. Lamy de la Chapelle, New insight into the aptamer conformation and aptamer/protein interaction by surface-enhanced Raman scattering and multivariate statistical analysis, Nanoscale, 2021, 13, 12443, DOI: 10.1039/d1nr02180j

[37] M. Vallejo-Perez, C. Ternon, N. Spinelli, F. Morisot, C. Theodorou, G. Jayakumar, P.-E. Hellström, M. Mouis, L. Rapenne, X. Mescot, B. Salem and V. Stambouli, Optimization of GOPS-Based Functionalization Process and Impact of Aptamer Grafting on the Si Nanonet FET Electrical Properties as First Steps towards Thrombin Electrical Detection, Nanomaterials 2020, 10, 1842, https://doi.org/10.3390/nano10091842

[38] X. Zeng, L. Zhang, X. Xiao, Y. Jiang, Y. Guo, X. Yu, X. Pu and M. Li, Unfolding mechanism of thrombinbinding aptamer revealed by molecular dynamics simulation and Markov State Model, Scientific reports, 6:24065 | DOI: 10.1038/srep24065

[39] C. Acquah, Y. W. Chan, S. Pan, L. S. Yon, C. M. Ongkudon, H. Guo and M. K. Danquah, Characterisation of aptamer anchored poly(EDMA-co-GMA) monolith for high throughput affinity binding, Scientific reports, (2019) 9:14501 https://doi.org/10.1038/s41598-019-50862- 1